LETTERS
https://doi.org/10.1038/s41558-018-0356-x
nature climate change

Increased snowfall over the Antarctic Ice Sheet mitigated twentieth-century sea-level rise

B. Medley[1*] and E. R. Thomas[2]

Changes in accumulated snowfall over the Antarctic Ice Sheet have an immediate and time-delayed impact on global mean sea level. The immediate impact is due to the instantaneous change in freshwater storage over the ice sheet, whereas the time-delayed impact acts in opposition through enhanced ice-dynamic flux into the ocean[1]. Here, we reconstruct 200 years of Antarctic-wide snow accumulation by synthesizing a newly compiled database of ice core records[2] using reanalysis-derived spatial coherence patterns. The results reveal that increased snow accumulation mitigated twentieth-century sea-level rise by ~10 mm since 1901, with rates increasing from 1.1 mm decade^{-1} between 1901 and 2000 to 2.5 mm decade^{-1} after 1979. Reconstructed accumulation trends are highly variable in both sign and magnitude at the regional scale, and linked to the trend towards a positive Southern Annular Mode since 1957[3]. Because the observed Southern Annular Mode trend is accompanied by a decrease in Antarctic Ice Sheet accumulation, changes in the strength and location of the circumpolar westerlies cannot explain the reconstructed increase, which may instead be related to stratospheric ozone depletion[4]. However, our results indicate that a warming atmosphere cannot be excluded as a dominant force in the underlying increase.

Annual accumulated snowfall over the grounded Antarctic Ice Sheet (AIS) amounts to ~6 mm of global sea-level equivalence; thus, both short- and long-term variations have a significant and direct impact on sea-level change. Global mean sea level (GMSL) is currently rising[5], but the overall contribution from the AIS remains poorly constrained[6]. Advances in satellite technology have vastly improved our understanding of ice-dynamic thinning and acceleration around the periphery of the ice sheet[6,7], yet the potential for ice-sheet-wide observations of snow accumulation fluctuations remains equivocal, designating mass input as arguably the largest source of uncertainty in AIS mass balance estimates. Modelling efforts have significantly reduced this knowledge gap[8], yet without any advancements in AIS accumulation observations, distinguishing between the varying abilities of the modelled net precipitation fields and assigning realistic uncertainties to them is not possible.

Atmospheric models suggest that snowfall over the AIS will probably rise as atmospheric warming increases its moisture-holding capacity[8]. Significant warming trends[9,10] over much of the Antarctica Peninsula and West AIS (WAIS) hint at the possibility of enhanced snowfall when considering thermodynamic changes alone. Surprisingly, investigation into this potential sea-level mitigation has received little attention, which we surmise stems from (1) the paucity of observed changes at appropriate spatiotemporal scales[11] and (2) the fact that observation-based atmospheric reanalysis data before the satellite era are not trustworthy[12]. The publication of research[11] indicating no substantial change in AIS snow accumulation between 1957 and 2005 nearly contemporaneously with a study[9] that found significant warming over much of the AIS, except portions of the East AIS (EAIS), suggests that the relationship between temperature and accumulation is more complex, and strongly supports the need for further study into recent AIS accumulation variability and its role in AIS contribution to GMSL.

Ice core records of snow accumulation, the combination of precipitation, sublimation/evaporation and deposition, wind redistribution and meltwater runoff provide enough temporal context (several decades to centuries) for trend evaluation, yet they fall short of sampling the entire AIS[2] and are noisy due to small-scale variability (for example, sastrugi)[13]. We use 'snow accumulation' over 'surface mass balance' because we are restricted to areas where surface mass balance is positive, which is the case for nearly the entire grounded AIS[14]. Atmospheric reanalyses provide spatiotemporally complete precipitation-minus-evaporation ($P-E$) products that are nearly equivalent to snow accumulation over the dry, grounded AIS, and are most trustworthy over the satellite era (1979–present). Notable biases in reanalysis $P-E$ exist[15,16]; however, they reproduce a significant portion of the interannual variability[17]. Here, we modify the methodology in ref. [11] to reconstruct nineteenth- and twentieth-century snow accumulation over the entire grounded AIS and surrounding islands using a combination of ice core records and atmospheric reanalysis $P-E$. A long-term, observationally based reconstruction of snow accumulation is necessary to: (1) ensure that any significant trends are observable over the noise; (2) quantify the role of AIS snow accumulation on observed sea-level change; (3) better quantify the relative importance of thermodynamic versus dynamic precipitation change; and (4) provide an AIS-wide observation-based snow accumulation record, along with uncertainties, for robust evaluation of global and regional atmospheric AIS net precipitation estimates.

Combining 53 ice core records with the spatial patterns of $P-E$ from 3 reanalyses, we reconstructed the 1801–2000 annual snow accumulation over the grounded AIS and surrounding islands (Fig. 1a, Supplementary Table 1 and Supplementary Figs. 1 and 2). We only show the results from reconstruction based on the Modern-Era Retrospective Analysis for Research and Applications Version 2 (MERRA-2) $P-E$ fields: R_{MERRA2}. The R_{MERRA2} performed better than the European Centre for Medium-Range Weather Forecasts 'Interim' (ERA-Interim)- and Climate Forecast System Reanalysis (CFSR)-based reconstructions (R_{ERAI} and R_{CFSR}, respectively) because: (1) the reanalysis showed the least bias in total magnitude (Supplementary Fig. 3); and (2) R_{MERRA2} exhibited the highest skill in reproducing the observations (see Supplementary Methods, Supplementary Fig. 4 and Supplementary Table 2). Here, we refer to the performance of the reconstruction and not the reanalysis product itself. In addition,

[1]Cryospheric Sciences Laboratory, NASA Goddard Space Flight Center, Greenbelt, MD, USA. [2]British Antarctic Survey, Cambridge, UK.
*e-mail: brooke.c.medley@nasa.gov

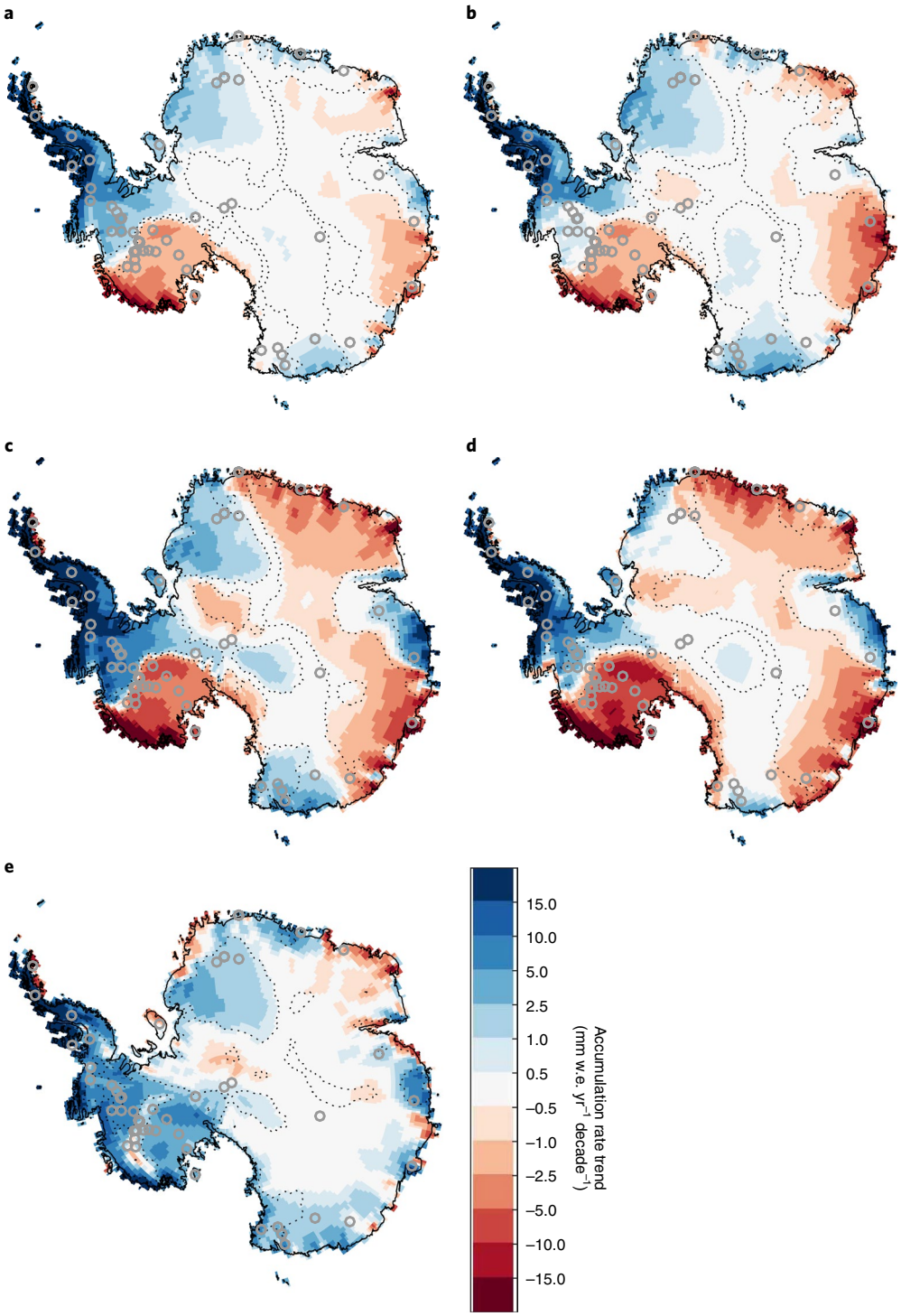

Fig. 1 | Trends in reconstructed Antarctic-wide snow accumulation and their relationship to the SAM. a–c, Absolute accumulation trends in mm of water equivalent (w.e.) per decade over 1901–2000 (**a**), 1901–1956 (**b**) and 1957–2000 (**c**), with regions of significance at the 1σ confidence level enclosed by the dashed lines. The grey open circles show ice core locations. **d**,**e**, The 1957–2000 SAM-congruent $P-E$ trend (**d**) is removed from the reconstructed trend in **c**, revealing the residual trend (**e**) that is not explained by the dominant mode of atmospheric variability in the high-latitude Southern Hemisphere.

we find that the reconstructions replicate a significant portion of the reanalysis $P-E$ variability between 1980 and 2000, even though a few of the ice cores used do not (Supplementary Fig. 5).

Trends in snow accumulation over the twentieth century (1901–2000) and late twentieth century (1957–2000) indicate that inhomogeneous patterns of change dominate any AIS-wide signal (Fig. 1a–c). They also suggest that mass is being significantly redistributed regionally over the AIS and has been since the 1957–1958 International Geophysical Year (and probably since the onset of the twentieth century). However, integrated over the entire ice sheet, we observe a clear and significant positive trend in snow accumulation (Fig. 2a). A steady increase is found over the EAIS, although it has reversed in the late twentieth century (Fig. 2b), even though local trends strengthened in the latter half (Fig. 1b).

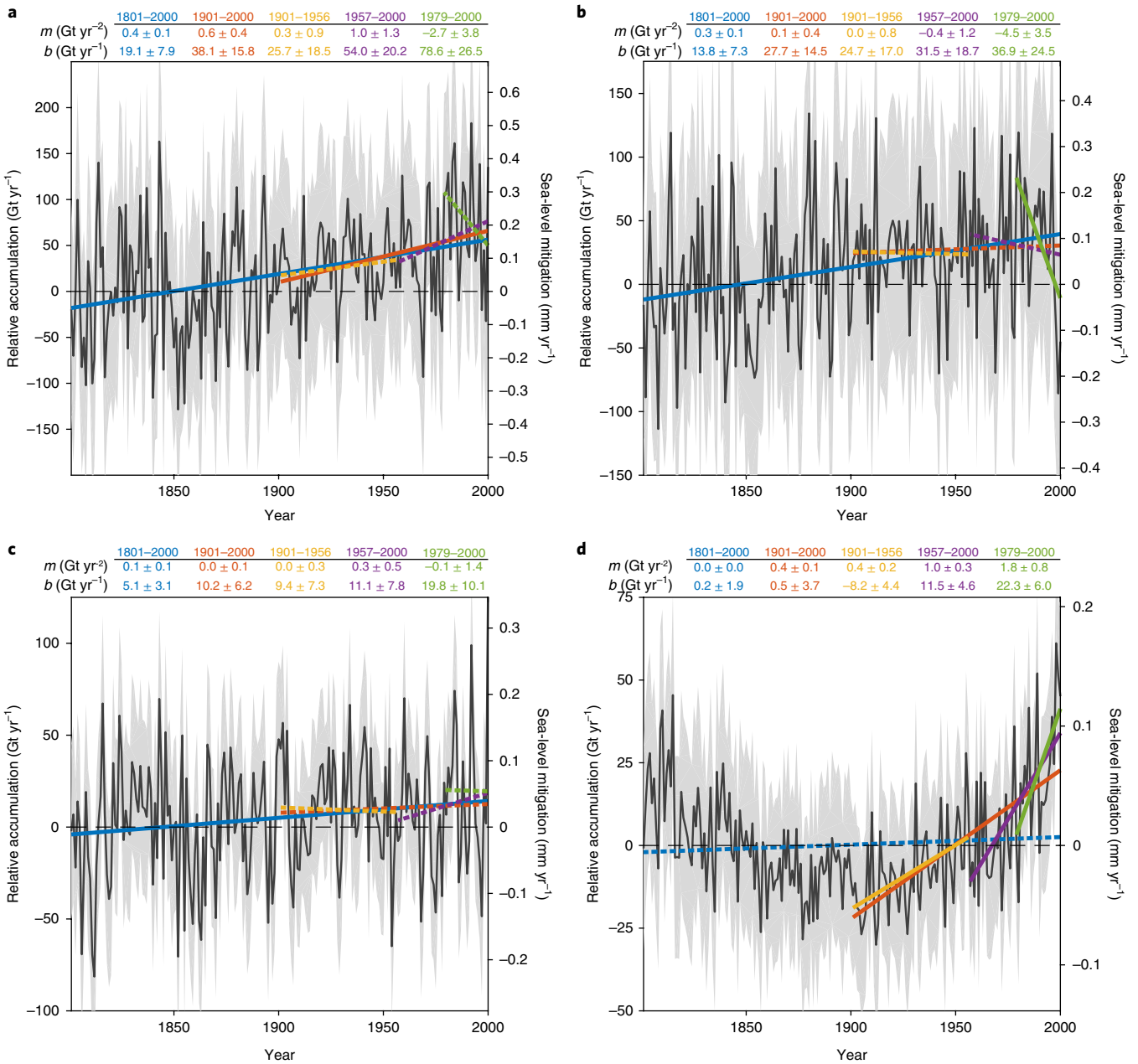

Fig. 2 | Nineteenth- and twentieth-century relative annual accumulation by Antarctic sector. a–d, Net accumulation over the AIS (**a**), EAIS (**b**), WAIS (**c**) and Antarctic Peninsula (**d**), relative to the nineteenth-century mean (dashed line). The shaded bounds are the 1σ uncertainties. The solid and dashed coloured lines represent significant and insignificant trends over various intervals, and the slope (*m*) and intercept (*b*) are included in a table above each time series (see 'Trend analysis' in the Methods).

We also observe a strong see-saw pattern of increased snow accumulation over the Antarctica Peninsula and eastern WAIS contrasted with decreased accumulation over the western WAIS. After nearly a century of decreasing snow accumulation over the Antarctica Peninsula, we find a rapid and potentially accelerating increase over the twentieth century (Fig. 2d), whereas the gains and losses from western and eastern WAIS largely balance (Fig. 2c). Because the reconstruction is spatiotemporally complete, we determine the net snow accumulation contribution to GMSL over the twentieth century by integrating the annual accumulation relative to the nineteenth-century mean (1801–1900; Fig. 2) through time.

Between 1901 and 2000, snow accumulation over the AIS and its peripheral islands mitigated GMSL by 1.12 ± 0.45 mm decade (dec)$^{-1}$; however, that rate more than doubled to 2.47 ± 0.76 mm dec^{-1} after 1979 (Fig. 3a). We determine that only the EAIS (0.77 ± 0.40 mm dec^{-1}) and WAIS (0.28 ± 0.17 mm dec^{-1}) mitigated GMSL over the twentieth century, but recent snow accumulation increases over the Antarctica Peninsula suggest that it will enter the twenty-first century as a source of significant GMSL mitigation (0.62 ± 0.17 mm dec^{-1}). Decreasing EAIS snow accumulation since 1979 indicates a potential slowdown in mitigation from this sector, while the opposite is true for the Antarctica Peninsula. It is critical to note that these sea-level mitigation values are based only on mass input to the AIS and do not account for the observed increases in mass output from glaciers that are in dynamic imbalance, such as Pine Island and Thwaites[6,18].

AIS-wide snow accumulation significantly mitigated twentieth-century GMSL, but did it result from thermodynamic or dynamic

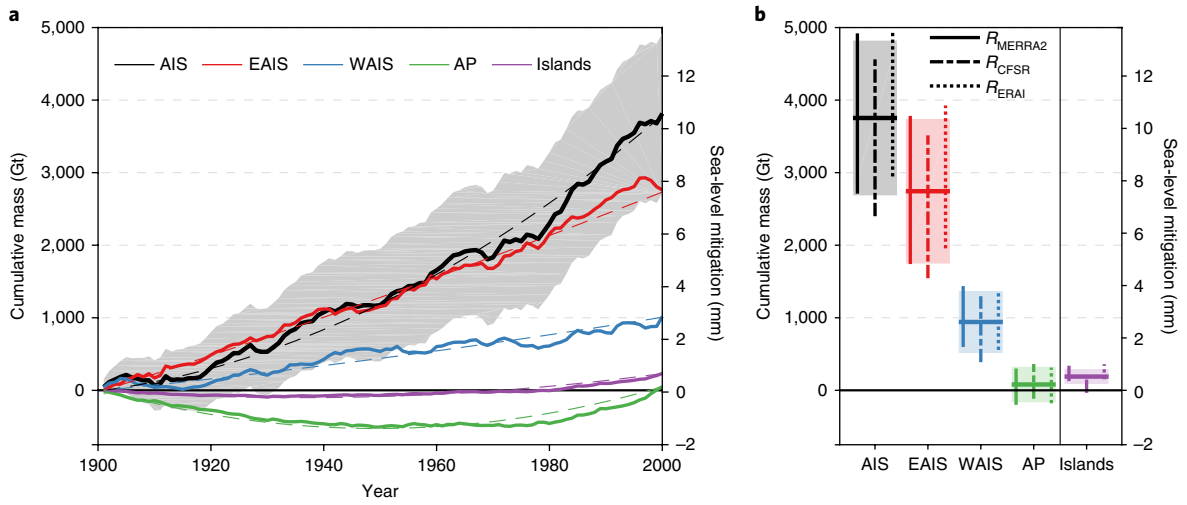

Fig. 3 | Twentieth-century cumulative mass and sea-level change due to snow accumulation. a, R_{MERRA2} cumulative mass and equivalent sea-level change by Antarctic sector over the twentieth century, relative to the nineteenth-century mean. The dashed lines represent a time-integrated model of mass change based on the linear regression statistics presented in Fig. 2. For clarity, the error bounds are included for the AIS only, and their derivation is described in the Methods section 'Sea-level mitigation'. **b**, Mass and sea-level mitigation by 2000 for each of the three reconstructions where the vertical lines show error bounds. The horizontal bar and shaded area represent the mean and combined uncertainty of all three reconstructions. All error bounds represent the ±1σ range. AP, Antarctica Peninsula.

precipitation change? The Southern Annular Mode (SAM), defined by a belt of low pressure surrounding the Antarctic that controls the strength and position of the circumpolar westerlies, is the dominant mode of atmospheric variability in the high-latitude Southern Hemisphere[19]. Since the 1957–1958 International Geophysical Year, the annual SAM index has exhibited a strong positive trend[3], largely due to anthropogenic ozone depletion and increased atmospheric greenhouse-gas concentrations[20], leading to a contraction of the belt of westerlies towards the Antarctic continent[21]. The pattern and magnitude of SAM-congruent trends and reconstructed snow accumulation trends are remarkably similar (Fig. 1c,d), indicating that changes in atmospheric circulation are a dominant force. Of note, we performed additional reconstructions after first removing the SAM-congruent $P-E$ signal from each reanalysis, and the results are nearly identical; thus, the pattern is independent and robust (see Supplementary Methods and Supplementary Figs. 6 and 7). Our reconstructions indicate that the positive SAM trend explains ~80% ($n>20{,}000$ and $P<<0.001$) of the spatial variability in the 1957–2000 trends, suggesting that anthropogenically driven atmospheric circulation changes are largely responsible for the snow mass redistribution over the AIS.

These findings are complicated by the simple fact that a positive trend in the SAM phase is accompanied by a negative trend in AIS-wide net precipitation in all three reanalyses. Thus, if an evolving SAM was solely responsible for the temporal trends in our reconstruction since 1957, we would expect that AIS-wide snow accumulation would contribute to sea-level rise rather than mitigate it. In fact, the SAM-congruent snow accumulation trend reduced the 1957–2000 GMSL mitigation by more than 2.5 mm.

Thus, we investigated the likelihood that the observed snow accumulation increases are due to atmospheric warming over the AIS. Investigation of the trend residuals (Fig. 1e) suggests that there are underlying positive snow accumulation trends over much of the AIS, especially coastal EAIS and most of WAIS and the Antarctica Peninsula (Supplementary Table 5). Because the positive trends are spatially pervasive, they are probably not attributable to changes in large-scale atmospheric circulation, which imparts a unique snowfall signature of often counteracting trends based on the relationship between wind anomalies and the regional topography[22]. Despite uncertainties in the reconstruction, as well as the SAM trend, the atmospheric warming required to account for the residual trends is consistent with modelling and observational efforts[9,10,23] (Table 1). Specifically, moderate temperature trends of 0.27, 0.17 and 0.06 °C dec^{-1} are needed over the Antarctica Peninsula, WAIS and EAIS, respectively. Strengthening or weakening of the positive trend in the SAM index shifts the warming between the Antarctica Peninsula and WAIS; thus, their combined warming remains nearly unchanged. Approximately 40% ($n>20{,}000$ and $P<<0.001$) of the spatial variability in the residual trends can be explained by the $P-E$ sensitivity to temperature, indicating that the regions most sensitive to temperature change are experiencing the largest changes. Thus, we cannot eliminate a warming atmosphere as the driver of the underlying snow accumulation increases.

A previous reconstruction found an insignificant negative trend in AIS-wide snow accumulation, suggesting that accumulation was not mitigating ice losses around the periphery and that atmospheric circulation variability, as opposed to thermodynamic moisture change, is the dominant driver[11]. We argue that our results are not incompatible with these findings. From a temporal standpoint, we find a positive, statistically insignificant trend (1.0 ± 1.3 Gt yr^{-2}) between 1957 and 2000; however, when the peripheral islands are included, the trend narrowly emerges as significant (1.4 ± 1.4 Gt yr^{-2}). Furthermore, our reconstruction is based solely on the ice core time series, whereas ref. [11] used ERA-40 $P-E$ from 1985–2005, which is the source of the negative trend. We use only observation-based values due to observing system artefacts in the reanalysis $P-E$ that compromise trend analysis[15]. Additionally, we find that circulation-driven precipitation change imparts a large signal on AIS-wide trends that are spatially heterogeneous, masking any underlying increases. Finally, we observe significant and insignificant decreasing trends over the EAIS (-4.5 ± 3.5 Gt yr^{-2}) and AIS (-2.7 ± 3.8 Gt yr^{-2}) since 1979, respectively, matching the trend sign in the previous reconstruction[11]. Thus, the differences in methodology, combined with the strength of the SAM-congruent snowfall signature, suggest that our results are not inconsistent with ref. [11].

While the temporal change in snow accumulation imparts a clear trend on GMSL mitigation, the spatial patterns of trend magnitude and sign have potential glaciological implications. Present-day rates of ice discharge across the grounding zone probably contain an

Table 1 | Temperature trends required to account for residual trends in reconstructed snow accumulation based on R_{MERRA2}

	Snow accumulation sensitivity to temperature (Gt °C^{-1})	Mean temperature trend (lower – upper quartile; °C dec^{-1})			1960–2005 temperature trends[10] (°C dec^{-1})				Twentieth-century temperature trends[23] (°C dec^{-1})
		SAM	SAM low	SAM high	NB14	M10	S09	O11	
AIS	233.3	0.08 (−0.01–0.16)	0.04 (−0.06–0.13)	0.11 (0.01–0.19)					0.04 ± 0.03–0.10 ± 0.09
EAIS	146.4	0.06 (−0.03–0.13)	0.02 (−0.07–0.11)	0.09 (0.01–0.16)	0.04 ± 0.12	0.10 ± 0.16	0.11 ± 0.12	0.05 ± 0.11	0.01 ± 0.12–0.04 ± 0.03
WAIS	64.9	0.17 (0.09–0.23)	0.12 (0.02–0.20)	0.20 (0.11–0.32)	0.19 ± 0.15	0.20 ± 0.16	0.16 ± 0.10	0.08 ± 0.09	0.06 ± 0.06–0.13 ± 0.09
AP	22.4	0.27 (0.07–0.35)	0.34 (0.16–0.44)	0.18 (−0.02–0.29)	0.29 ± 0.19	0.39 ± 0.22	0.11 ± 0.07	0.30 ± 0.13	0.11 ± 0.06–0.29 ± 0.11
Islands	11.6	0.15 (0.01–0.28)	0.20 (0.02–0.37)	0.10 (−0.05–0.22)					
AIS + islands	245.0	0.08 (−0.01–0.16)	0.05 (−0.05–0.14)	0.11 (0.01–0.19)					
WAIS + AP	87.3	0.18 (0.09–0.23)	0.15 (0.03–0.22)	0.20 (0.09–0.32)					

The snow accumulation sensitivity to near-surface air temperature is provided. Mean temperature trends are the area-weighted mean over each sector, and the lower- and upper-quartile bounds by area are shown in parentheses. Temperature trends from four reconstructions over a similar time interval from ref. [10] and reconstructed twentieth-century trends from ref. [23] are shown. AP, Antarctica Peninsula.

atmospherically driven component that varies in scale and direction depending on its location[1]. We demonstrate that ice mass is being significantly redistributed across the AIS, highlighting the need for improved understanding of expected atmospherically driven ice-dynamic changes to isolate regions of change that exceed this surface climate signal.

Evaluation of our 200-year reconstruction of AIS-wide snow accumulation suggests that climate-change-related dynamic and potentially thermodynamic forces probably control the observed spatiotemporal trends, with the dynamic forces outweighing thermodynamic forces since 1957, masking the underlying positive snow accumulation trends. We cannot eliminate atmospheric warming as the source of snow accumulation GMSL mitigation, especially considering that the temperature trends necessary to account for the residual snow accumulation trends are similar to temperature reconstructions. Recent work[4] suggests that increased snow accumulation since the mid-twentieth century might be attributable to stratospheric ozone depletion. However, a mechanistic link was not uncovered, exposing the complexity of the relationship between ozone depletion, the strength and location of the circumpolar westerlies, air temperature, and ultimately accumulation.

Modern-day accumulation over the AIS is 78.6 ± 26.5 Gt yr^{-1} higher than the nineteenth-century mean—a value more than 1.5 times the AIS rate of mass loss during the 1990s[24]. Nevertheless, net AIS mass loss[24] (2,720 ± 1,390 Gt) over just 26 years (1992–2017) has accounted for 70% of the century-long snow accumulation gains (3,815 ± 1,105 Gt). An insignificant negative trend in AIS snow accumulation hints at the possibility of a reduction in annual mass gain after 2000; however, even if it is frozen at 78.6 Gt yr^{-1}, snow accumulation gains are a mere one-third of the AIS mass losses (219 ± 43 Gt yr^{-1}), indicating that snow accumulation is not keeping pace with oceanic-driven ice mass loss.

Online content

Any methods, additional references, Nature Research reporting summaries, source data, statements of data availability and associated accession codes are available at https://doi.org/10.1038/s41558-018-0356-x.

Received: 17 May 2018; Accepted: 13 November 2018;
Published online: 10 December 2018

References

1. Winkelmann, R., Levermann, A., Martin, M. A. & Frieler, K. Increased future ice discharge from Antarctica owing to higher snowfall. *Nature* **492**, 239–242 (2012).
2. Thomas, E. R. et al. Review of regional Antarctic snow accumulation over the past 1000 years. *Clim. Past Discuss.* **2017**, 1–42 (2017).
3. Marshall, G. J. Trends in the Southern Annular Mode from observations and reanalyses. *J. Clim.* **16**, 4134–4143 (2003).
4. Lenaerts, J. T. M., Fyke, J. & Medley, B. The signature of ozone depletion in recent Antarctic precipitation change: a study with the Community Earth System Model. *Geophys. Res. Lett.* https://doi.org/10.1029/2018GL078608 (2018).
5. Beckley, B. et al. Assessment of the Jason-2 extension to the TOPEX/Poseidon, Jason-1 sea-surface height time series for global mean sea level monitoring. *Mar. Geod.* **33**, 447–471 (2010).
6. Shepherd, A. et al. A reconciled estimate of ice-sheet mass balance. *Science* **338**, 1183–1189 (2012).
7. Pritchard, H. D., Arthern, R. J., Vaughan, D. G. & Edwards, L. A. Extensive dynamic thinning on the margins of the Greenland and Antarctic ice sheets. *Nature* **461**, 971–975 (2009).
8. Palerme, C. et al. Evaluation of current and projected Antarctic precipitation in CMIP5 models. *Clim. Dynam.* **48**, 225–239 (2017).
9. Steig, E. J. et al. Warming of the Antarctic ice-sheet surface since the 1957 International Geophysical Year. *Nature* **457**, 459–462 (2009).
10. Nicolas, J. P. & Bromwich, D. H. New reconstruction of Antarctic near-surface temperatures: multidecadal trends and reliability of global reanalyses. *J. Clim.* **27**, 8070–8093 (2014).
11. Monaghan, A. J. et al. Insignificant change in Antarctic snowfall since the International Geophysical Year. *Science* **313**, 827–831 (2006).
12. Schneider, D. P. & Fogt, R. L. Artifacts in century-length atmospheric and coupled reanalyses over Antarctica due to historical data availability. *Geophys. Res. Lett.* **45**, 964–973 (2018).
13. McConnell, J. R., Mosley-Thompson, E., Bromwich, D. H., Bales, R. C. & Kyne, J. D. Interannual variations of snow accumulation on the Greenland Ice Sheet (1985–1996): new observations versus model predictions. *J. Geophys. Res. Atmos.* **105**, 4039–4046 (2000).
14. Van Wessem, J. M. et al. Modelling the climate and surface mass balance of polar ice sheets using RACMO2: part 2: Antarctica (1979–2016). *Cryosphere* **12**, 1479–1498 (2018).
15. Bromwich, D. H., Nicolas, J. P. & Monaghan, A. J. An assessment of precipitation changes over Antarctica and the Southern Ocean since 1989 in contemporary global reanalyses. *J. Clim.* **24**, 4189–4209 (2011).
16. Palerme, C. et al. Evaluation of Antarctic snowfall in global meteorological reanalyses. *Atmos. Res.* **190**, 104–112 (2017).
17. Medley, B. et al. Airborne-radar and ice-core observations of annual snow accumulation over Thwaites Glacier, West Antarctica confirm the spatiotemporal variability of global and regional atmospheric models. *Geophys. Res. Lett.* **40**, 3649–3654 (2013).
18. Medley, B. et al. Constraining the recent mass balance of Pine Island and Thwaites glaciers, West Antarctica, with airborne observations of snow accumulation. *Cryosphere* **8**, 1375–1392 (2014).
19. Thompson, D. W. & Wallace, J. M. Annular modes in the extratropical circulation. Part I: month-to-month variability. *J. Clim.* **13**, 1000–1016 (2000).
20. Arblaster, J. M. & Meehl, G. A. Contributions of external forcings to southern annular mode trends. *J. Clim.* **19**, 2896–2905 (2006).
21. Van Den Broeke, M. R. & Van Lipzig, N. P. Changes in Antarctic temperature, wind and precipitation in response to the Antarctic Oscillation. *Ann. Glaciol.* **39**, 119–126 (2004).
22. Fyke, J., Lenaerts, J. T. & Wang, H. Basin-scale heterogeneity in Antarctic precipitation and its impact on surface mass variability. *Cryosphere* **11**, 2595–2609 (2017).
23. Stenni, B. et al. Antarctic climate variability on regional and continental scales over the last 2000 years. *Clim. Past* **13**, 1609–1634 (2017).

24. Shepherd, A. et al. Mass balance of the Antarctic Ice Sheet from 1992 to 2017. *Nature* **556**, 219–222 (2018).

Acknowledgements
We acknowledge everyone involved in the collection and analysis of the ice core records used in our reconstruction, as well as A. Barker and J. Lenaerts for manuscript comments. B.M. and E.R.T. were supported by NASA's ICESat-2 Project Science Office and the British Antarctic Survey (Natural Environment Research Council), respectively.

Author contributions
Both authors designed the study. B.M. wrote the manuscript with input from E.R.T. E.R.T. analysed the ice core records. B.M. performed the reconstruction and its analysis thereafter.

Competing interests
The authors declare no competing interests.

Additional information
Supplementary information is available for this paper at https://doi.org/10.1038/s41558-018-0356-x.

Reprints and permissions information is available at www.nature.com/reprints.

Correspondence and requests for materials should be addressed to B.M.

Publisher's note: Springer Nature remains neutral with regard to jurisdictional claims in published maps and institutional affiliations.

Methods

Snow accumulation over the grounded AIS and its surrounding islands was reconstructed on the premise that the variability at a specific location has an associated spatial signature (that is, regions with a direct and indirect coherence). While distance is probably a factor here, we must recognize the complex interaction of topography and predominant wind direction in generating orographic effects not controlled by distance alone. Therefore, we used modelled spatial signatures from atmospheric reanalysis $P-E$ as the basis of our interpolation weighting scheme. Because of their aforementioned ability to reproduce the interannual variability[17], which strengthens the weighting scheme, we used global atmospheric reanalyses over regional climate models.

The reconstruction method applied here is an improvement on a previous study[11] that provides sufficient detail to replicate the work; thus, we only briefly describe the methodology and our modifications. Rather than rely on a single reanalysis model, we generated three reconstructions based on different atmospheric reanalyses, including ERA-Interim, MERRA-2 and CFSR (see below), whereas ref. [11] relied only on ERA-40. In such a manner, we created three reconstructions, where each used the same ice core observations but different modelled spatial weights, giving no preference to a specific model. The reanalyses have different observing and assimilation systems and spatial grids; therefore, it is only reasonable to expect site-specific spatial signatures to vary to some extent.

Our validation analysis of the reconstructions was very thorough and is thus detailed in the Supplementary Methods.

Global atmospheric models. We created annual $P-E$ products from three global atmospheric reanalysis products—specifically, ERA-Interim[25], the National Aeronautics and Space Administration (NASA) MERRA-2[26] and the National Centers for Environmental Prediction CFSR[27]. Specifically, we used ERA-Interim monthly means of twice-daily 12 h forecast accumulations of total precipitation and evaporation, MERRA-2 monthly mean total precipitation and evaporation, and CFSR monthly mean of 6 h forecast accumulations of total precipitation and 6 h averages of latent heat flux, which were converted to sublimation using the latent heat of sublimation (2,838 kJ kg^{-1}).

The CFSR data were the combination of two versions of CFSR: version 1 spans 1979–2010 and version 2 spans 2011–2016. We repeated the reconstruction using only version 1 data, but the results did not vary significantly. To keep consistency with the ERA-Interim and MERRA-2 reanalyses, we used the combined CFSR record (1979–2016).

The modelled spatial signatures were based on the full reanalysis time period (1979–2016 for ERA-Interim and CFSR, and 1980–2016 for MERRA-2) using $P-E$ time series normalized to the overlapping period with all ice core records (1980–1988). Normalization ensured that all measurements were relative to the same interval, while basing the signatures on the full reanalysis time period provided as long a climatological context as possible for the reconstruction. Similar to ref. [11], we generated spatial weights for each ice core by calculating its shared variance with all locations via the coefficient of determination (r^2).

Ice core data. We used 53 annually resolved ice core records of snow accumulation that cover a substantial portion of the AIS and a few surrounding islands (Supplementary Fig. 1). The majority of these records are available in a newly compiled database[2]. Of the 80 records in ref. [2], we used 52 for the reconstruction (Supplementary Table 1). We required that each record spanned the 1980–1988 period to provide several years of overlap with the reanalyses and to maximize the number of cores used in the reconstruction (Supplementary Fig. 2). We also excluded several records that did not exhibit fully annual resolution throughout the entire record, which came largely from the early site survey for the European Project for Ice Core Drilling in Dronning Maud Land. One newly published record was added to the dataset: the B40 record[28]. The maximum correlation at each grid point with the reanalysis-based $P-E$ at each ice core site indicated that the ice core coverage was very good, especially over West Antarctica and the Antarctic Peninsula (Supplementary Fig. 8). Weaker correlations over the high plateau suggested that we would benefit from additional observations from these locations. However, accumulation rates were so low over the East Antarctic plateau that it was extremely challenging to create an annually resolved record.

Unlike ref. [11], we opted to include all records, whether they spanned the full reconstruction interval (1801–2000) or not. Only 16 records spanned the entire interval, and coverage was not sufficient to fully capture the accumulation variability, especially over the EAIS and Antarctica Peninsula (Supplementary Fig. 8). Under our premise, the minimum number of records used was 29 for any year (Supplementary Fig. 2). On the basis of the distribution of records that existed at the beginning (1801) and end (2000) of our reconstruction interval, we captured the common variability (Supplementary Fig. 8).

To assess our ability to reconstruct the variability, we performed an additional reconstruction using the $P-E$ values directly from the reanalysis in a 'best-case' scenario. For each year of the reconstruction, we used the reanalysis $P-E$ records for the given ice core combination and attempted to reconstruct the entire reanalysis $P-E$ field. In such a manner, we could assess the proportion of variability explained at each grid cell under each ice core combination, providing insight into our ability to capture AIS-wide accumulation variability. Supplementary Table 3 contains the accumulation-weighted expected proportion of variance explained over the entire record and over the different sectors. The results indicate that we are typically able to explain about 61% of the variance in AIS snow accumulation over the entire 200-year interval; however, this proportion dips slightly to 59 and 51% for 1801 and 2000, respectively. Thus, we conclude that even with gaps in our ice core network, we are consistently able to capture a large portion of the variability in AIS-wide snowfall.

To ensure that we did not introduce spurious artefacts in our reconstructed trends, we also performed a cross-validation reconstruction using only the 16 complete records. This was termed the ComplCore reconstruction. We found that the trends in the full and ComplCore reconstructions were similar, and this is explained in more detail in the Supplementary Methods.

Reanalysis $P-E$ bias. The atmospheric reanalysis $P-E$ products exhibited biases in total magnitude across much of the AIS that varied substantially from one another[15]. Using observations of annual surface mass balance from the ice core data presented above, radar-derived measurements over the Pine Island and Thwaites glacier catchments[18], and an AIS-wide database[29] of surface mass balance, we assessed the magnitude bias in the three reanalyses used in our study (Supplementary Fig. 3). Although it limited our spatial coverage, we only used observations from ref. [29] that fell within (and only within) the reanalysis period (1979/80–2016). The surface mass balance values were then compared with the modelled $P-E$ from the grid cell to which they belonged for the contemporaneous years, bias = (model−observation)/model. If multiple observations existed for a single grid cell, they were averaged together to create one bias correction per cell. In such a manner, we found the relative errors in the modelled $P-E$ magnitudes that were then interpolated over the entire AIS using the statistical interpolation method of kriging (that is, distance-based interpolation).

Bias correction can potentially influence our results since change is calculated relative to the mean annual accumulation. Thus, if the bias correction is incorrect (or incomplete), the quality of the estimated sea-level impact is compromised. To assess whether to use the bias-corrected reconstructions, we compared the validation statistics from the bias- and non-bias-corrected reconstructions for R_{MERRA2}, R_{ERAI} and R_{CFSR}. The final reconstructions were bias corrected for R_{MERRA2} and R_{ERAI} and non-bias corrected for R_{CFSR} because these reconstruction scenarios outperformed the others. Mitigation values by the year 2000 were very similar between the final reconstructions (R_{MERRA2}: 10.6 mm; R_{ERAI}: 11.0 mm; R_{CFSR}: 9.7 mm), suggesting that the reconstructed trends are similar even though the actual magnitudes are different (Fig. 3b). We determined that R_{MERRA2} is the most robust since it exhibits the least bias in magnitude (Supplementary Fig. 3); that is, sea-level mitigation from the bias- and non-bias-corrected R_{MERRA2} reconstructions are very similar at 10.6 and 10.8 mm, respectively.

Reconstruction error analysis. We generated gridded annual uncertainty for the reconstructed accumulation rates by accounting for both measurement error (that is, small-scale variability or noise in the ice core records) and the uncertainty introduced by the spatial sampling of cores. While modelled $P-E$ is often biased over the AIS, it can reproduce the interannual variability with some skill[17]. At the same time, trends in reanalysis products are sometimes untrustworthy as shifts in the observing system can generate spurious jumps through time[15]. Therefore, we assessed the noise (or uncertainty) in each ice core record by calculating the root mean square error (RMSE) between the detrended record and the reanalysis time series at the grid cell corresponding to the location of the ice core. We assigned the final uncertainty for each record as the minimum of the standard deviation of the reanalysis time series and RMSE. These values comprised the observational uncertainty in units of normalized accumulation and were propagated through on a cell-by-cell and year-by-year basis.

Accounting for the uncertainty introduced by limited spatial sampling is extremely important. A reconstruction based on two ice core records will have a much larger uncertainty than one based on tens of records, and that uncertainty will vary in space. To determine the uncertainty due to the sampling geometry of the cores, we performed the reconstruction a second time, replacing the ice core time series with the reanalysis time series from each of the ice core sites. Essentially, we assessed our ability to recreate the reanalysis $P-E$ records over the entire AIS using only a subset of reanalysis time series that corresponded to the locations of the ice core records. This uncertainty varied with time as the number of cores used in the reconstruction varied in time. Specifically, we determined the spatiotemporal RMSE of this reanalysis-based reconstruction by comparing it with the actual reanalysis data. These values comprised the sampling errors in units of normalized accumulation. The final uncertainty product was the square root of the sum of squares of the two sources of uncertainty (observation and sampling errors).

Spatial integration. To determine mass change on a cell-by-cell basis, we scaled the grid-cell snow accumulation (mm w.e. yr^{-1}) by the area of the grounded ice within the grid cell. The sectors are defined by the basins in ref. [30]: the EAIS basins were 2–17 (10.1×10^6 km^2); WAIS basins were 1 and 18–23 (1.8×10^6 km^2) and the Antarctica Peninsula basins were 24–27 (0.2×10^6 km^2). The entire AIS (12.2×10^6 km^2) and surrounding islands (0.2×10^6 km^2) were defined by the

Moderate Resolution Imaging Spectroradiometer mosaic of Antarctica grounded ice and islands vector datasets[31,32], and their combination represents the total area of grounded ice in the Antarctic (12.4×10^6 km^2).

To generate the sector time series, we combined the mass time series over the entire area of each spatial region of interest. The associated uncertainty time series accounts for the spatial correlation of grid-cell time series (that is, highly correlated, dependent records yield higher uncertainties than if all the records were entirely independent of one another): rather than taking the square of the sum of the square errors, we scaled the uncertainties by the correlation (or dependence) of each pair of records. In such a manner, we accounted for the fact that many of the cells within a spatial region of interest were based primarily on the same core records, reducing their independence and thus increasing their uncertainties.

Trend analysis. To determine the trends in snow accumulation and their associated uncertainties, we used a Monte Carlo method to generate $n=10{,}000$ simulations of the 1801–2000 sector-integrated time series of snow accumulation (Fig. 2) by adding random noise to the original time series that was normally distributed with a mean of zero and standard deviation equal to the propagated uncertainty. We then calculated the trend of each realization with time zeroed at the middle of the time interval of interest, providing an intercept approximately equal to the mean of the time series over that interval. Our final trends and intercepts (Fig. 2) and their respective errors were the mean and standard deviation of all of the realizations. The intercept (Gt yr^{-1}) represents the mean annual relative snow accumulation over the period of interest. If this is positive and significant, it indicates that the sector is mitigating sea-level rise over that time interval. The slope (Gt yr^{-2}) is an indicator of whether mitigation from a given sector is undergoing an acceleration. These regression statistics represent a simple model of snow accumulation behaviour, and when integrated, provide the modelled sea-level mitigation curves in Fig. 3.

Sea-level mitigation. To evaluate the role of AIS snow accumulation on twentieth-century sea-level change, we assumed that nineteenth-century mass input via snow accumulation is representative of the long-term mean for an AIS in balance. This choice is justified by the fact that out of the 28 records that extend beyond the nineteenth century, 23 have nineteenth-century mean annual accumulation rates equal to the mean over the entire record based on a two-sample two-tailed Student's t-test with 95% confidence ($300\leq$ d.f. $\leq 2{,}155$). Therefore, nineteenth-century accumulation is probably a tenable substitute for a longer-term (several-century) mean in the absence of sufficient observations. Cumulative mass change is determined by accumulating the relative annual snow accumulation (Fig. 2) with time, which is then converted to sea-level equivalence by dividing by 361 Gt.

To determine the rates of sea-level mitigation and their uncertainties, we used a Monte Carlo method to generate $n=10{,}000$ simulations of the 1801–2000 sector-integrated time series of snow accumulation (Fig. 2) by adding random noise to the original time series that was normally distributed with a mean of zero and standard deviation equal to the propagated uncertainty. Next, we determined the cumulative mass change of each realization, where the uncertainty (shaded area in Fig. 3) was the standard deviation of the simulated cumulative mass time series. Such a method allowed us to capture the impact of uncertainty in the nineteenth-century mean annual snow accumulation rather than relying solely on the regression statistics from 1901 onwards that are presented in Fig. 2.

SAM-congruent trends. We estimated the SAM-congruent trends in snow accumulation by first assessing the $P-E$ sensitivity to deviations in the SAM. After calculating the reanalysis-based SAM index[33], we performed cell-by-cell linear regression between the detrended $P-E$ and SAM time series. Unfortunately, the reanalyses began in 1979/80, so to get a longer-term perspective on the role of an evolving SAM, we used a proxy-based SAM index[3] that extended back to 1957. The $P-E$ sensitivity to the SAM was next multiplied by the 1957–2000 SAM index trend (0.59 ± 0.20 dec^{-1}), providing the SAM-congruent trend in $P-E$ (Fig. 1d). To evaluate residuals, we removed the SAM-congruent trend signal from our reconstruction (Fig. 1e). The patterns and magnitudes are robust across all three reanalysis reconstructions (Supplementary Fig. 10), as well as the RemoveSAM cross-validation reconstructions.

***P*−*E* sensitivity to air temperature.** We assessed $P-E$ sensitivity to the 2 m air temperature through linear regression of their detrended time series on a cell-by-cell basis, providing the change in $P-E$ for every degree change in temperature. While these models showed spurious trends and shifts in temperature[15], we were purely exploiting the relationship between temperature and accumulation. We found that the three models have similar sensitivities over the AIS (ERA-Interim: 192 Gt °C^{-1}; MERRA-2: 233 Gt °C^{-1}; CFSR: 264 Gt °C^{-1}), with MERRA-2 falling in the middle, which is potentially because ERA-Interim and CFSR $P-E$ values are biased low and high, respectively. Next, we divided the residual trends in Fig. 1e by the $P-E$ sensitivity to temperature to estimate the temperature trend required to explain reconstructed trends that are not attributable to the SAM. We present the area-weighted mean associated temperature trends over each sector in Table 1. To account for uncertainty in the trend in the SAM index, we performed the same exercise using the upper (SAM high) and lower (SAM low) 1σ trend bounds.

Code availability

The code for generating the reconstructions is available from the NASA Goddard Cryosphere data portal (https://neptune.gsfc.nasa.gov/csb/).

Data availability

The snow accumulation reconstructions generated and analysed during this study are available from the NASA Goddard Cryosphere data portal (https://neptune.gsfc.nasa.gov/csb/). The reanalysis data are available as follows: CFSR (https://rda.ucar.edu/pub/cfsr.html), ERA-Interim (https://www.ecmwf.int/en/forecasts/datasets/archive-datasets/reanalysis-datasets/era-interim) and MERRA-2 (https://disc.gsfc.nasa.gov/). The ice core records are hosted at https://ramadda.data.bas.ac.uk/repository/entry/show?entryid=83f2ca40-04b5-4029-a04c-c18b202dc2f8.

References

25. Dee, D. P. et al. The ERA-Interim reanalysis: configuration and performance of the data assimilation system. *Q. J. R. Meteorol. Soc.* **137**, 553–597 (2011).
26. Gelaro, R. et al. The Modern-Era Retrospective Analysis for Research and Applications, Version 2 (MERRA-2). *J. Clim.* **30**, 5419–5454 (2017).
27. Saha, S. et al. The NCEP Climate Forecast System Reanalysis. *Bull. Am. Meteorol. Soc.* **91**, 1015–1057 (2010).
28. Medley, B. et al. Temperature and snowfall in western Queen Maud Land increasing faster than climate model projections. *Geophys. Res. Lett.* **45**, 1472–1480 (2018).
29. Favier, V. et al. An updated and quality controlled surface mass balance dataset for Antarctica. *Cryosphere* **7**, 583–597 (2013).
30. Zwally, H. J., Giovinetto, M. B., Beckley, M. A. & Saba, J. L. *Antarctic and Greenland Drainage Systems* (GSFC Cryospheric Sciences Laboratory, 2012).
31. Haran, T., Bohlander, J., Scambos, T., Painter, T. & Fahnestock, M. *MODIS Mosaic of Antarctica 2008–2009 (MOA2009) Image Map* Version 1 (National Snow and Ice Data Center, 2014); https://doi.org/10.7265/N5KP8037
32. Scambos, T. A., Haran, T. M., Fahnestock, M. A., Painter, T. H. & Bohlander, J. MODIS-based Mosaic of Antarctica (MOA) data sets: continent-wide surface morphology and snow grain size. *Remote Sens. Environ.* **111**, 242–257 (2007).
33. Gong, D. & Wang, S. Definition of Antarctic Oscillation index. Geophys. Res. Lett. **26**, 459–462 (1999).